

RECENT MACHINE STUDIES AND IMPROVEMENTS OF THE CERN ANTI-PROTON ACCUMULATOR

G. Carron, V. Chohan, T.W. Eaton*, C.D. Johnson, E. Jones, H. Koziol, M. Martini, S. Maury, C. Metzger, F. Pedersen, A. Poncet, L. Rinolfi, T.R. Sherwood, C.S. Taylor, L. Thorndahl, S. van der Meer, and E.J.N. Wilson
European Laboratory for Particle Physics (CERN)
CH-1211 Geneva 23

Abstract

Numerous machine studies and improvements of the CERN Antiproton Accumulator¹, mostly during the period from January 1984 to August 1986, when the ACOL² installation shutdown started, are presented. Some were aimed at immediate improvements in performance such as higher stacking rate, lower core emittances, or operational flexibility. Others were aimed at a better understanding of problems related to antiproton intensity in preparation for the higher stack intensities expected after completion of the ACOL project in 1987.

Introduction

Many different aspects of the CERN Antiproton Accumulator affect the overall average production rate of antiprotons delivered to the AA "clients": ISR (until June 1984), LEAR, and SPS³.

The primary intensity of the 26 GeV/c p-production beam from the PS, and the target zone configuration (spot size, target material, collector lens) affects the p-source brightness. For a given brightness, the effective injection acceptance of the AA determines the number of antiprotons collected on injection orbit. Losses which occur during precooling, RF capture and deposit, and during stack-tail momentum cooling reduce the number of new p's pushed into the stack core to little over half of those injected. This rate, minus the intensity dependent stack-loss rate, gives the stack accumulation rate. When p's are unstacked and transferred to the PS, the direct ejection and transfer losses are augmented by the indirect losses resulting from stopping the stacking for eventual cooldown prior to transfer.

Finally the reliability of the AA complex influences the average production rate.

The core emittances during stacking are important for efficient LEAR transfers, since the transfer efficiency from PS to LEAR after deceleration in PS can be very poor if the emittance is too large. There

will be an indirect accumulation loss if there has to be a cooldown period prior to each transfer. The limiting core emittances after cooldown for an antiproton transfer to the SPS collider (typically every 24 hours) have a direct influence on luminosity, and a smaller influence on the transfer efficiency than in the case of the more frequent transfers to LEAR.

Several stack intensity related instabilities have been studied and most of these cured. Some are longitudinal (interaction with stochastic cooling systems and the RF system), while others are transverse (due mostly to interaction with ions).

Machine studies addressing each of the factors mentioned above are summarised below.

Production Rate Related Subjects

The factors affecting the average production rate are:

- 1) Intensity of primary 26 GeV/c proton beam.
- 2) Target zone configuration.
- 3) Effective AA acceptance.
- 4) Precooling efficiency.
- 5) RF capture and deposit efficiency.
- 6) Stack-tail efficiency.
- 7) Stack loss rate.
- 8) Unstacking and ejection efficiency.
- 9) Availability (reliability).

The primary proton beam intensity went up from about 1.1×10^{13} p's per pulse on target in Autumn 1983 to 1.5×10^{13} in 1985 and 1986, with a peak of 1.65×10^{13} during a machine study session. These intensities require, however, a lot of delicate fine tuning in both the PS Booster and the PS and are usually only available several weeks after start-up.

With few exceptions, the standard target zone configuration⁴ used in operation consists of a pulsed quadrupole triplet for primary beam focusing, a $\emptyset 3 \times 120$ mm Cu target supported in graphite and enclosed in

Table I Experimental target zone configurations.

Date	Primary Beam Lens	Target	Collector lens	Rel. Yield	Remarks
-	Pulsed quadrupoles	$\emptyset 3 \times 120$ mm Cu in C	Horn	1.0	Normal operation
09/83	Pulsed quadrupoles	$\emptyset 3 \times 100$ mm Cu in C, 140 kA	Horn	1.5	2 h test (failure)
09/83	Pulsed quadrupoles	$\emptyset 3 \times 60$ mm W	2 cm Li-lens (500 kA)	1.4	Yield test only
06/84	2 cm Li-lens	$\emptyset 3 \times 110$ mm CuBe in C, 70 kA	Horn	1.4	2 h test (failure)
10/84	2 cm Li-lens	$\emptyset 3 \times 120$ mm Cu	Horn	1.05	6 week test (OK)
03/85	2 cm Li-lens	$\emptyset 3 \times 115$ mm Ag in Al ₂ O ₃ , 100 kA	Horn	1.4	2 h test (failure)
07/85	2 cm Li-lens	$\emptyset 3 \times 115$ mm Fe in Al, 100 kA	Horn	1.25	1 h test (OK)
08/85	Pulsed quadrupoles	$\emptyset 3 \times 60$ mm Re	2 cm Li-lens (420 kA)	1.30	4 week test (failures)

* Sheffield City Polytechnic, GB-Sheffield.

an air-cooled Al container, and a coaxial magnetic horn of short focal length for focusing the emerging 3.5 GeV/c negative secondaries. Several other target zone configurations (Li-lenses, high-density targets, axial pulsed current targets) with higher p/p yields have been tested⁵⁻⁷ (Table I). The improvements in p/p yield are normalised to the standard copper target and horn configuration. None of these experimental configurations have demonstrated the excellent reliability of the Cu target-horn configuration with a working life in excess of 1 year. There is, however, a degradation in yield of ~20% during the first two weeks of operation of a new copper target. This is believed to be caused by void formation and swelling⁷⁻⁸, an effect well known from studies of radiation damage to nuclear reactor materials. The failures of the experimental set-ups are analysed in ref. 7.

The configuration planned for initial operation of ACOL in 1987 consists of a short, high-density, water-cooled iridium target followed by a 2 cm Li-lens. Remote handling, independent access, and a nearby hot-cell will make the ACOL target area much better suited for operation with more complex and less reliable target zone components.

Reshimming of the AA quadrupoles and closed orbit corrections by moving quadrupoles have resulted in improved ring optics. Acceptances close to the design acceptance ($A_H = A_V = 100\pi$ mm.mrad) were finally obtained: $A_H \approx 98\pi$, $A_V \approx 78\pi$ across the 6% momentum aperture, combined with small tune variations and small dispersion in the zero dispersion straights (Fig. 1). In addition, much smaller local chromaticities and dispersion were obtained in the core region for reasons which will be explained later.

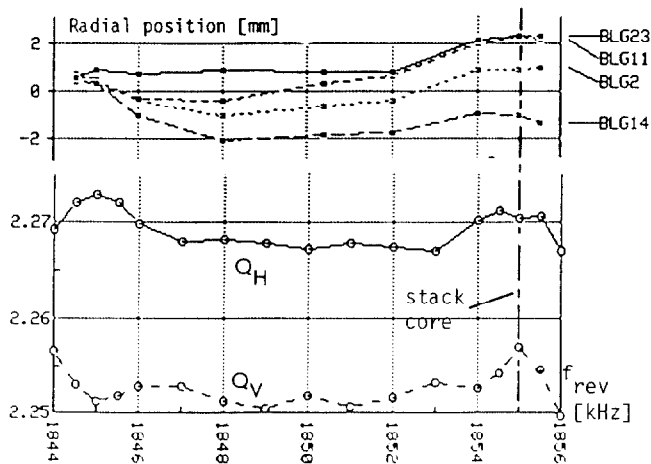


Fig. 1 - Tunes and radial position versus momentum.

Injection of p's into this aperture is facilitated by automatically setting the septum and kicker from observation of the phase and amplitude of the coherent oscillations of injected electrons. This proves to be a method which optimises the yield well when the standard target zone layout is used⁹, less so when a Li-lens is used as collector lens.

The observed relative depopulation of phase space at large amplitudes⁹ (particles with simultaneously large amplitudes in both planes are missing) has been shown to be caused by linear and non-linear coupling between the two planes and partly cured by choosing a tune for accumulation away from the diagonal, and adding a skew quadrupole and two sextupoles in the zero dispersion straights¹⁰. The sextupoles

improved the injection and accumulation yields by 12-20%. Attempts to visualise the betatron amplitude modulation associated with the non-linear coupling by observing the coherent motion of a small test bunch failed since we are not equipped in the AA to inject a test bunch with simultaneously large amplitudes in both planes, but the method will be pursued in the AC ring.

The momentum precooling pick-up ferrites were replaced by 4E3 material in 1983 which gave a significant improvement in signal to noise ratio and thus in momentum precooling performance. In 1984 a substantial effort was devoted to improving the precooling efficiency by improving the filter response so as to minimise the transverse heating (causing loss since the aperture is filled), but not much was gained. Typical precooling efficiency is 72-75%, with the precooling losses about equally distributed between the three planes: Δp , H, V.

The RF capture and deposit efficiency is ~90% and agrees closely with the capture efficiency expected from measuring the momentum distribution after precooling. Only a few percent are lost during the deceleration from injection orbit to stack tail orbit. Simulations and experiments showed that an unsuitable choice of vector lengths in the function generators controlling the RF¹¹ could excite synchrotron oscillations of harmful amplitudes. This was avoided by suitable vector lengths in the RF function generator.

The stack-tail efficiency is defined as the ratio between the antiproton flux deposited by the RF in the tail and the sum of stacking rate and stack-loss rate (measured with stack-tail momentum cooling off). At low stack intensities ($< 5 \cdot 10^{10}$) this efficiency is 85-95%, and depends on the number of production cycles in the PS supercycle.

At a stack intensity of $5 \cdot 10^{11}$ p's the stacking rate has dropped by as much as 40%. The origin of this loss in stacking rate is a drop in stack-tail efficiency. Several machine experiments indicate that they are caused by a stack intensity dependent excitation of ion-induced non-linear resonances¹² of 15th order several of which are crossed in the tail region (Fig. 2).

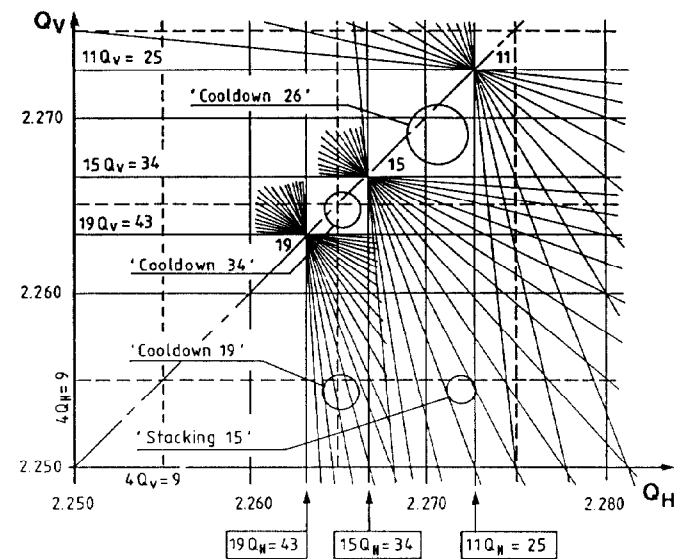


Fig. 2 - Tune diagram.

The stack loss rate is normally dominated by single Coulomb and nuclear scattering on residual gas nuclei. With $5 \cdot 10^{-11}$ torr and 90% H₂ the lifetime is

about 3000 h. Even at the highest stack intensities (the record is $5.23 \cdot 10^{11}$) the loss rate is only a few percent of the stacking rate. However, several abnormal situations can increase this loss rate substantially.

1) Common mode overlap (see below) in the 1-2 GHz transverse core cooling system, causing a loss rate up to 20% of stacking rate.

2) Ion induced non-linear resonances¹²⁻¹³, in particular $11Q_H + 4Q_V = 34$ and $11Q_H = 25$, if the core tune values are allowed to drift (Fig. 2).

3) Single Coulomb and nuclear scattering from captured, solid microparticles¹²⁻¹⁴. The loss rate often exceeds the stacking rate.

The unstacking and ejection efficiency is normally ~95% if the core emittances are below 4π mm. mrad. An undesirable side effect of the reshimming and orbit correction session in March 1985 was a reduction of the ejection acceptance to $\sim 1\pi$. The obstacle was located between the kicker and the septum, and was easily corrected by displacing one end of the RF cavity.

Intentional interruption of stacking for cooldown prior to transfer may seriously deteriorate the effective unstacking and ejection efficiency when the lost stacking time is taken into account. This is not important for SPS transfers once a day, where a one hour cooldown prior to transfer only represents a small fraction, but a serious problem for efficient deliveries to LEAR every $1\frac{1}{2}$ h. Prior to 1984, core emittances during stacking were so large that stacking was done during the night, while only transfers were done during the day, resulting in an effective reduction of p-production by 50%. Hence the interest in maintaining low core emittances during stacking which allow p-transfers with only a few minutes interruption.

The availability of the AA is given in Table II with and without accidental stack loss taken into account. Accidental loss of stacks is accounted for as down-time by converting the number of p's lost into stacking time.

Table II AA availability.

	1984	1985	1986
Excl. stack loss	94.5%	93.8%	96.2%
Incl. stack loss	86.9%	83.1%	90.8%

Access to the AA hall and the target zone without dumping the stack will be possible after ACOL, and should reduce the frequency of dumping for access. The longest continuously circulating p-stack was kept for 999 h (42 days) in Autumn 1985.

Core Emittance Related Subjects

The factors influencing the core emittances are:

- 1) Common mode overlap.
- 2) Stack-tail momentum kicker symmetry.
- 3) Dispersion at stack-tail kicker.
- 4) Stack-tail momentum cooling noise.
- 5) Multiple Coulomb residual gas scattering.
- 6) Intrabeam scattering.
- 7) Ion-induced non-linear resonances.
- 8) Ion-antiproton coherent instabilities.
- 9) Charged solid microparticles.
- 10) The stochastic cooling system.
- 11) RF overlap knock-out.

The first four effects are only present during stacking, while the last is only present during unstacking.

Common mode overlap results in transverse heating when the stack distribution is sufficiently wide for partial overlap between longitudinal and transverse frequencies from particles with different momenta within the stochastic cooling bandwidth, and in presence of longitudinal (common mode) signals above the noise level. Prior to 1983 the transverse stack core cooling pick-up was located in a dispersive region¹⁵ causing off-momentum particles to produce large common mode signals in the horizontal system. The new transverse core cooling pick-up in a dispersion-free straight improved upon this, but the residual common mode signal was large enough to cause some harm when the stack was wide enough for the overlap condition to exist. This occurs during stacking. Particles in the tail are excited by signals from the core, and vice versa. Also the widening of the core momentum distribution during stacking due to noise in the stack-tail momentum cooling system causes the high-frequency edge of the core to overlap with the low-frequency edge and vice versa. The amplitude of the common mode was reduced by careful centering of the beam in the pick-up by moving the beam, the pick-up, or both, by improving the symmetry, reducing reflections (e.g. feedthroughs), and adding damping resistors to attenuate wave-guide propagation. From 1985 and onwards the high core loss rates induced by common mode overlap during stacking disappeared.

After switching to the new transverse core cooling pick-up in 1983, the stack-tail momentum kicker asymmetry was identified as the dominant stack-core heating mechanism during stacking, and the bad kicker modules identified. Fixing bad or missing connections in Spring 1984 reduced the heating enough to permit 24 h/day operation for LEAR, but certain kicker modules were still bad enough to justify a complete overhaul to improve their symmetry in January 1986. This resulted in very low vertical heating rates, while most of the remaining horizontal heating was identified as being caused by residual dispersion at the supposedly dispersion-free location of the stack-tail kicker, and at the core momentum. The reshimming in March and May 1986 reduced the residual dispersion at the core momentum by one order of magnitude.

The heating rates from the 1-2 GHz slot type momentum kicker were measured with beam followed by lab measurements of its symmetry in view of its future use as stack-tail kicker after the ACOL installation in the band 0.9-2.4 GHz.

The stack-tail momentum cooling noise causes dilution of the core momentum distribution during stacking, which in itself is not harmful, but results in transverse heating when combined with common mode overlap, and makes the core occupy a larger area in the tune diagram making it more difficult to locate the core between resonances. The pick-up noise has been reduced by cooling the pick-up termination resistors¹⁵ to 20°K and is further reduced by notch filters.

Multiple Coulomb scattering on residual gas nuclei is normally about one order of magnitude less important than intrabeam scattering¹⁶ at typical stack densities, but can become significant in case of abnormal pressure and gas composition.

The multiple Coulomb intrabeam scattering was expected to be the main and most fundamental horizontal and longitudinal heating effect. Good agreement has been obtained between experiments and calculation¹⁶ for intense p-stacks, and relatively low-intensity

p-stacks, but excessive transverse heating rates have been observed for high-intensity p stacks, an effect which is attributed to heating by ion-induced non-linear resonances¹²⁻¹³.

These resonances are harmful at stack intensities above 10^{11} p's. The heating is reduced during stacking by carefully locating the dense core between two 15th order resonances (Fig. 2), which requires careful tune control ($\pm 10^{-4}$) and very small local chromaticities. During cooldown it is further reduced by changing the core tune to an area clear of resonances up to 19th order, "cooldown 19". The reshimming in March 1985 flattened the tunes across the momentum aperture with the purpose of locating the entire working line clear of the 15th order resonances, but too much was lost in injection yield from non-linear coupling by working closer to the diagonal, and we returned to the usual stacking tune. Interruption in the use of the UA1 detector permitted p-stacks between 3×10^{11} and 5×10^{11} in April and May 1986. Above 2.5×10^{11} several isolated 19th order resonances could be observed at the "cooldown 19" tune as localised heating in the Schottky sidebands at 1.5 GHz, and a systematic search for a better cooldown tune was undertaken. Transverse heating rates E_{HM} and E_{VM} were measured and compared with the rates E_{HC} and E_{VC} calculated from intrabeam scattering¹⁶. The ratio between measured and calculated rates is given in Table III for the horizontal plane where the heating is strongest. "Cooldown 26" and "cooldown 34" are clear of resonances up to 26th and 34th order, respectively (Fig. 2).

Table III Relative horizontal heating versus tune.

Tune	Intensity pbars	$E_{H,AV}$ mm.mrad	$E_{V,AV}$ m.mmrad	E_{HM}/E_{HC}
Stacking 15	3.01×10^{11}	10.8π	3.7π	33.3
Cooldown 19	2.49×10^{11}	4.3π	1.6π	9.5
Cooldown 19	5.18×10^{11}	9.5π	2.9π	11.8
Cooldown 26	3.68×10^{11}	5.1π	1.9π	5.3
Cooldown 26	4.89×10^{11}	7.2π	2.8π	6.6
Cooldown 34	2.49×10^{11}	2.9π	1.3π	3.6
Cooldown 34	4.11×10^{11}	5.6π	2.3π	3.8

The excessive heating is attributed to ion-induced non-linear resonances, still harmful in spite of steady improvements and additions to the electrostatic clearing system.

Ion-antiproton coherent instabilities¹² limit the minimum vertical emittance during cooldown for intensities between 1.5×10^{11} and 4×10^{11} p's. Above 4×10^{11} the present core cooling system is unable to cool down to the threshold emittance due to ion-induced non-linear resonances and intrabeam scattering. Improvements to the clearing system have lowered the growth rate. A dedicated vertical pick-up resonating at the lowest n-Q_v betatron sideband has been built and allowed detailed studies of the instability as well as attempts to damp the fast growing instability by high gain feedback.

Charged solid microparticles¹²⁻¹⁴ provoke very fast emittance growth when present due to multiple Coulomb scattering in the very intense electric field surrounding the microparticle. They may usually be eliminated successfully by slowly cycling the clearing field, but can prevent stacking or antiproton transfer for many hours if the elimination procedure is not

successful. Improvements to the clearing system should provide a more reliable elimination procedure in the future besides lowering the number of uncleared potential well pockets where microparticles may be trapped.

The performance of the core cooling system, in particular the bandwidth, is important since faster cooling rates will result in lower equilibrium core emittances. Space was liberated in dispersion-free straight section 13 for a 4-8 GHz kicker for transverse core cooling and a 2-4 GHz kicker for momentum core cooling needed for the higher stack intensities expected after the ACOL installation. This was done by feeding the three existing 1-2 GHz core cooling signals into a single slot kicker structure instead of two. The Ap signal, split in two by a matched T-junction, was fed into the previously terminated sum ports of the two hybrids feeding the slot kicker in the two differential modes. The 4-8 GHz was installed in January 1986, beam tests began in March, and in July horizontal cooling of an antiproton stack of 5.3×10^{10} was observed with a time constant of 9 minutes compared with 30 minutes for the old 1-2 GHz system.

RF overlap knock-out¹⁷, first observed in the ISR, was initially a problem during unstacking of triple dense transfers to SPS ($3 \times 10\%$ of stack). It is caused by overlap of the higher harmonics of the unstacked bunch frequency and core betatron sidebands. It was cured by keeping the RF voltage low while the frequency is changing so as to reduce the high-harmonic content of the spectrum.

Intensity Related Instabilities

All intensity related instabilities which are or have been troublesome are listed below:

Longitudinal coherent instabilities:

- 1) Stack-tail momentum pick-up parasitic coupling to core.
- 2) Precooling pick-up parasitic coupling to core.
- 3) Phase loop instabilities.
- 4) RF cavity impedance.

Transverse coherent instabilities:

- 5) Resistive wall instabilities.
- 6) Electron-proton instabilities.
- 7) Ion-antiproton instabilities.

Transverse incoherent instabilities:

- 8) Ion-induced non-linear resonances.
- 9) Capture of solid microparticles.

The stack-tail momentum pick-up parasitic coupling to core¹⁵ results in longitudinal instabilities of the core via the high-gain stack-tail momentum cooling system. It widens the core momentum distribution, or requires lower than optimum stack-tail gain at high stack intensities. It was originally believed to be caused by propagating TE modes excited by vertical asymmetries. However, improvements to the vertical symmetry in 1984 did not reduce the undesired coupling. It was found that a better ground connection of the coax line between tank feedthrough and the inner structure raised the instability threshold to acceptable levels.

The momentum precooling pick-up parasitic coupling to core creates similar problems, and was reduced to a harmless level by improved RF connections to the core shielding screens around those pick-ups.

The phase loop instability¹¹ is due to an increased apparent impedance of the RF system seen by the core during unstacking through action of the phase loop. It is cured by reduction of phase loop gain and appropriate programming of the RF function for unstacking.

The effect is worst when the ratio of stack to unstacked intensity is high, but as low as 0.3% of the stack intensity has been reliably unstacked for LEAR.

The longitudinal coupling impedance of the AA ring has been measured by observing the instability threshold of narrow momentum slices unstacked from a dense core and then debunched. This was investigated as function of the operational state of the RF cavity (Table IV).

Table IV Longitudinal coupling impedance.

Z/n	Cavity state (h = 1)
500 Ω	on tune, feedback on (normal)
1600 Ω	off tune, feedback off (off)
28 k Ω	on tune, feedback off

The first value is due to AA ring structures other than the RF cavity, since the cavity impedance seen by the beam has been reduced to Z/n = 200 Ω by RF feedback¹¹, while the following two values are due to the RF cavity.

The second value is still a safe value for most stacks and permits switching the RF cavity off for repairs without losing the stack, while the third value will make most stacks unstable and has caused several partial losses of stack until an interlock was installed to prevent this state.

All transverse resistive wall instabilities (coasting, bunched head-tail, proton, antiproton) are successfully damped by a bidirectional transverse feedback damping system¹⁸.

Electron-proton instabilities¹⁹⁻²⁰, first observed in the ISR, appear during cooling studies with intense test proton stacks, and result in a high vertical heating rate. They disappear if the vacuum is good and the clearing system is switched to reversed polarity (positive).

The three remaining instabilities have all been discussed in the previous chapter.

Conclusions

During the last three years we have considerably extended our understanding of the many effects which limit the performance of the Antiproton Accumulator. The target brightness has been pushed to the limit set by the ability of suitable target materials to withstand the thermal shock of an intense proton beam. The optics of the AA ring itself has been honed to produce a dynamic aperture which is 80% of the mechanical space within the vacuum chamber. A whole class of effects due to one cooling system feeding signals to another through harmonics of beam frequencies common to both, has been analysed and, to a large extent, eliminated. Yet another class of effects which lead to emittance growth has been identified as due to uncleared ions and their interaction with the antiproton stack. Surprisingly, non-linear resonances of an order as high as 34 can be driven by this ion-beam effect which resembles the beam-beam effect in a collider.

Having uncovered the various limiting phenomena we are currently replacing almost all the cooling systems of the AA to cater for the higher fluxes that the new AC ring will deliver to AA later this year. We are also currently installing improved ion-clearing systems and fast feedback systems to handle instabilities at the expected higher stack densities. No doubt

the new AA will yield yet another crop of intriguing phenomena.

References

- [1] Design Study of a Proton-Antiproton Colliding Beam Facility, CERN/PS/AA/78-3, 1978.
- [2] E.J.N. Wilson (Editor), "Design Study of an Antiproton Collector for the Antiproton Accumulator", CERN 83-10, 1983.
- [3] The PS Staff, "The CERN PS Complex as an Antiproton Source", *IEEE Trans. Nucl. Sci.*, Vol. NS-30, p. 2039, 1983.
- [4] E. Jones et al., *IEEE Trans. Nucl. Sci.*, Vol. NS-30, p. 2778, 1983.
- [5] T.W. Eaton et al., "Conducting Targets for Antiproton Production of ACOL", *IEEE Trans. Nucl. Sci.*, Vol. NS-32, No.5, pp.3060-3062.
- [6] D.C. Fiander et al., "Beam Tests of a 2 c Lithium Lens", *IEEE Trans. Nucl. Sci.*, Vol. NS-32, p. 3063, 1985.
- [7] T.W. Eaton et al., "Recent Work on the Production of Antiprotons from Pulsed Current Targets", CERN/PS/86-15 (AA), 1986.
- [8] T.W. Eaton, Private Communication.
- [9] C.D. Johnson, "Antiproton Yield Optimisation in the CERN Antiproton Accumulator", *IEEE Trans. Nucl. Sci.*, Vol. NS-30, p. 2821, 1983.
- [10] V. Chohan et al., "Antiproton Losses at Large Transverse Amplitudes in the CERN Antiproton Accumulator and Corrective Measures Using Skew Quadrupoles and Sextupoles", *IEEE Trans. Nucl. Sci.*, Vol. NS-32, p. 2231, 1985.
- [11] R. Johnson et al., "Measuring and Manipulating an Accumulated Stack of Antiprotons in the CERN Antiproton Accumulator", *IEEE Trans. Nucl. Sci.*, Vol. NS-30, p. 2290, 1983.
- [12] E. Jones et al., "Transverse Instabilities due to Beam-Trapped Ions and Charged Matter in the CERN Antiproton Accumulator", *IEEE Trans. Nucl. Sci.*, Vol. NS-32, p. 2218, 1985.
- [13] A. Dainelli, "Antiproton-Positive Ion Transverse Instabilities in the CERN Antiproton Accumulator", CERN/PS/87-13 (AA), 1987.
- [14] F. Pedersen, this Conference.
- [15] G. Carron et al., "Recent Experience with Antiproton Cooling", *IEEE Trans. Nucl. Sci.*, Vol. NS-30, p. 2587, 1983.
- [16] M. Martini, *Intrabeam Scattering in the ACOL-AA Machine*, CERN/PS/84-9 (AA), 1984.
- [17] J.P. Gourber et al., *IEEE Trans. Nucl. Sci.*, Vol. NS-24, p. 1405, 1977.
- [18] F. Pedersen et al., "Tackling Transverse Coherent Instabilities of Co and Counter Rotating Beams in the CERN Antiproton Accumulator", *IEEE Trans. Nucl. Sci.*, Vol. NS-30, p. 1343, 1983.
- [19] H.G. Hereward, CERN 71-15, 1971.
- [20] E. Keil and B. Zotter, ISR-TH/71-58, 1971